



Modelling the interplay between the CD4⁺/CD8⁺ T-cell ratio and the expression of MHC-I in tumours

Christian John Hurry¹ · Alexander Mozeika² · Alessia Annibale^{1,3}

Received: 1 July 2020 / Revised: 24 April 2021 / Accepted: 26 May 2021 /
Published online: 18 June 2021
© The Author(s) 2021

Abstract

Describing the anti-tumour immune response as a series of cellular kinetic reactions from known immunological mechanisms, we create a mathematical model that shows the CD4⁺/CD8⁺ T-cell ratio, T-cell infiltration and the expression of MHC-I to be interacting factors in tumour elimination. Methods from dynamical systems theory and non-equilibrium statistical mechanics are used to model the T-cell dependent anti-tumour immune response. Our model predicts a critical level of MHC-I expression which determines whether or not the tumour escapes the immune response. This critical level of MHC-I depends on the helper/cytotoxic T-cell ratio. However, our model also suggests that the immune system is robust against small changes in this ratio. We also find that T-cell infiltration and the specificity of the intra-tumour TCR repertoire will affect the critical MHC-I expression. Our work suggests that the functional form of the time evolution of MHC-I expression may explain the qualitative behaviour of tumour growth seen in patients.

Keywords CD4/CD8 ratio · MHC-I · Immunology · Statistical mechanics

CJH is supported by the Engineering and Physical Sciences Research Council Centre for Doctoral Training in Cross-Disciplinary Approaches to Non-Equilibrium Systems (CANES, EP/L015854/1).

✉ Christian John Hurry
christian.hurry@kcl.ac.uk

Alexander Mozeika
alexander.mozeika@kcl.ac.uk

Alessia Annibale
alessia.annibale@kcl.ac.uk

¹ Department of Mathematics, King's College London, Strand, London WC2R 2LS, UK

² London Institute for Mathematical Sciences, Royal Institution, 21 Albemarle Street, London W1S 4BS, UK

³ Institute for Mathematical and Molecular Biomedicine, King's College London, Hodgkin Building, London SE1 1UL, UK

Mathematics Subject Classification MSC 37C25 · MSC 82C99 · MSC 37N25 · MSC 92B99

1 Introduction

It is now known that tumours evoke an immune response, which can alter the growth and makeup of a tumour. Greater understanding of the anti-tumour immune response has led to the development of immunotherapies, which have seen some degree of success in clinical trials, particularly in cancers of the blood (Kochenderfer et al. 2014; Brentjens et al. 2013; Leach et al. 1996; McDermott et al. 2015; Hodi et al. 2010). However, the use of these therapies in solid cancers and conversion to the clinic still remains a challenge as was pointed out by Kakarla and Gottschalk (2014).

The immune system can be seen as a network of interacting cells, with many different cell types working together to perform a wide-ranging and robust function against pathogens. In addition to this, tumours are rapidly evolving parts of this network. A systemic understanding of the mechanisms of the anti-tumour immune response is, therefore, vital in the development of immunotherapies. Immediately, this questions what should be considered important systemic processes and what can be regarded as non-dominant behaviour. With this in mind this paper seeks to address the adaptive, T-cell dependent anti-tumour immune response.

T-cells are lymphocytes, a group of white blood cells, distinguished from other lymphocytes by their unique receptor known as the T-cell receptor (TCR). A TCR is specific to a particular antigen (a part of a protein recognised by a TCR). In addition to this, T-cells can be split into two main sub-types: helper and cytotoxic T-cells. Antigens are picked up by professional antigen presenting cells (APCs) and presented as a peptide on the surface molecule MHC-II. Helper T-cells can then activate by binding to MHC-II which displays the antigen that the TCR is specific to. Activated helpers can then activate cytotoxic T-cells which eliminate cells that present their conjugate antigen via MHC-I. The T-cell dependent response eliminates infected cells, but is also invoked by tumours (Restifo et al. 2012).

A common experimental technique in immunology is immunostaining, which uses antibodies that bind to specific proteins, to sort cells. Helper T-cells are known for their high expression of the protein CD4, and cytotoxic cells for high CD8. For this reason, they are commonly referred to as CD4⁺ and CD8⁺ cells, respectively. A decrease in the CD4⁺/CD8⁺ ratio is considered to be a good prognostic marker for conditions associated with immunodeficiency such as HIV (Taylor et al. 1989; Serrano-Villar et al. 2014), and aging (Wikby et al. 1998; Olsson et al. 2001).

Solid tumours are a porous mixture of tumour cells, immune cells and healthy tissue cells. T-cells can infiltrate tumours and the CD4⁺/CD8⁺ ratio of infiltrating T-cells can be measured from tumour samples. A low CD4⁺/CD8⁺ of infiltrating T-cells has been considered as a marker for prognosis across several cancer types including: cervical (Sheu et al. 1999), breast (Sheu et al. 2008; Sevcíková et al. 1992), lung, liver, testicular and colorectal cancers (Tancini et al. 1990). Tancini et al. (1990) surveyed tumours from a cohort of breast, lung, colorectal, liver and testicular cancers, and found that low intra-epithelial CD4⁺/CD8⁺ was associated with early stage cancer

due to an expanded CD8⁺ population, and that later stage cancers were associated with low CD4⁺/CD8⁺ due to a loss of the CD4⁺ population. In addition to these results in solid cancers, a low CD4⁺/CD8⁺ ratio in the blood correlated with poor survival in chronic lymphocytic leukemia (CLL) (Nunes et al. 2012). Despite the evidence that across cancer types a low CD4⁺/CD8⁺ ratio is a sign of poor prognosis, patients with a low CD4⁺/CD8⁺ ratio of tumour infiltrating T-cells were found to have significantly improved survival in separate studies of colorectal cancer (Diederichsen et al. 2003) and ovarian cancer (Sato et al. 2005), contradicting these studies.

There are many factors, biological and immunological, which could account for the prognostic variability in the CD4⁺/CD8⁺ ratio. Overall T-cell infiltration, i.e the density of T-cells in a tumour, may account for this variability in tumours, as the absolute number of T-cells will affect the strength of the immune response. As one would expect, the density of T-cells has also been shown to correlate with prognosis in cancer (Ménard et al. 1997; Ryschich et al. 2005). However, recent results have shown that the tumour reactivity of infiltrating T-cells, which reflects the proportion of TCRs that are specific to tumour associated antigens, is low in cancers where infiltration is a marker for prognosis (Scheper et al. 2019). Therefore, the infiltration of specific T-cells may also lead to variability in prognostic markers.

A key stage in the progression of tumours is the down-expression of MHC-I, a cell surface molecule with which immune cells interact (Garcia-Lora et al. 2003). Despite evidence for MHC-I expression correlating with prognosis, the relationship with tumour growth is less clear. The total absence of MHC-I in breast tumours has been shown to activate a group of innate immune cells, natural killer (NK) cells, which can kill cells without MHC-I recognition (Madjd et al. 2005). However, studies of colorectal cancer showed that tumours with high MHC-I were found in patients with longer survival times and that MHC-I could be used as an independent marker of prognosis (Watson et al. 2006; Simpson et al. 2010). To complement the results seen with breast cancer, the total absence of MHC-I in colorectal cancer also showed longer patient survival times compared with low MHC-I expression, due to the activation of NK cells (Watson et al. 2006). To summarise, MHC-I expression impacts the growth of tumours *in vivo*, with low expression favouring tumour growth, while high expression leading to longer patient survival. The exception is tumours with an absence of MHC-I which trigger an innate immune response from NK cells. This stresses the importance of tumour heterogeneity: low MHC-I expression, due to a large proportion of cells down-expressing MHC-I, will prevent a sufficient T-cell response, but the low level of MHC-I will also interrupt the response from NK cells.

There is a mechanistic interplay between the CD4⁺/CD8⁺ ratio and MHC-I expression. This is because cytotoxic cells, which form the majority of CD8⁺ cells, bind to MHC-I in order to eliminate tumour cells. In spite of this fact there is a lack of data measuring the CD4⁺/CD8⁺ ratio and MHC-I together. One study has shown that the prognostic value of T-cell markers improves when MHC-I expression is also considered (Turcotte et al. 2014). Additionally, the loss of MHC-I in pancreatic cancer has been shown to lead to a lower level of infiltration by cytotoxic T-cells (Ryschich et al. 2005). Cytotoxic T-cell infiltration was found to be a marker of prognosis, however, MHC-I alone was not. Our hypothesis is that the interplay between CD4⁺/CD8⁺, T-cell infiltration, and MHC-I could explain the differences in prognostic value for

these parameters across individual tumours and different cancers. To address this we create a mathematical model, starting from known cellular processes to derive system-wide behaviour. The aim is to see if such a model captures this interplay and explains potential variation in the prognostic value of $CD4^+/CD8^+$ and MHC-I.

As research has turned towards systemic modelling of the immune system there has been an increase in mathematical and computational approaches to modelling challenges in immunology. Mathematical models used are mainly *deterministic*, comprised of ordinary differential equations (ODEs). Such models usually fall into two extremes: either, the model is low dimensional, ‘macroscopic’, and does not fully capture the systemic behaviour of the system; or it is high dimensional, ‘microscopic’, with a large number of unknown parameters; usually this makes statistical evaluation of these models with real data difficult. Furthermore, ODE models also fail to capture the inherent *stochasticity* of biological processes. In this paper we consider a model that lies between these two approaches, keeping the model to a few key parameters, whilst also including inherent stochasticity of microscopic behaviour.

The cytotoxic anti-tumour response has been modelled previously, most notably by Kuznetsov et al. (1994). Despite their pioneering efforts, they neglected to include the immunosuppressive effects of the tumour microenvironment, something which was later accommodated for by Dritschel et al. (2018) who included specifically the interactions between the helper and cytotoxic T-cell populations. Both models are deterministic and our work deviates from them in this respect.

In our work we model the interplay between the $CD4^+/CD8^+$ T-cell ratio and the expression of MHC-I in tumours explicitly. Although our model is also a system of ODEs which describe the change in concentration of cells, our model differs from previous efforts by including the stochastic dynamics of T-cell activation. The latter is used in the derivation of our model, but our analysis is based on non-equilibrium statistical mechanics, as similarly implemented by Annibale et al. (2018), allowing us to describe the macroscopic behaviour of the system deterministically. Statistical mechanics has a rich recent history in modelling the immune system (Perelson and Weisbuch 1997; Lucia and Maino 2002; Chakraborty and Košmrlj 2010; Mora et al. 2010; Agliari et al. 2013; Bartolucci et al. 2016) and here we use it to address the unique modelling challenges that tumour immunology poses. In doing so we derive a condition for the eradication of tumours which reveals a critical threshold of MHC-I expression. This threshold is found to depend on the $CD4^+/CD8^+$ T-cell ratio, T-cell infiltration, and T-cell specificity.

In this work, we exclude the effects of NK cells and macrophages, focusing exclusively on the T-cell dependent response. This allows our model to be kept to a few key parameters that can be analysed in full. As previously discussed, NK cells play a dominant role when MHC-I is totally *absent*, a case which is less relevant for our model. The role of macrophages in the tumour is a double edged sword, with macrophages eliminating tumour cells, and also forming part of the bulk tumour. This behaviour is complex, and has been modelled elsewhere (Eftimie and Eftimie 2018), and is unlikely to affect our analysis on the interplay between the $CD4^+/CD8^+$ T-cell ratio and MHC-I. The result of this work is a low dimensional model with just a few important parameters, derived from known immunological and biological mechanisms.

The remaining sections of this paper will be organised as follows: in Sec. 2 we will introduce our mathematical model for tumour-immune interactions, in Sec. 3 we will present four key results that are of biological relevance and we will provide a discussion that assesses how our results fit in with the questions raised by the literature. We will discuss benefits and limitations of our modelling approach as well as pathways for future work in Sec. 4. Technical details are described in the appendix.

2 Constructing a mathematical model

2.1 The adaptive anti-tumour immune response

The anti-tumour immune response can be described by a series of cellular kinetic rate reactions. Here we list the full set of reactions that we model. By describing the immune response in this way, we can use the law of mass action to write a series of ODEs for further analysis. We consider the anti-tumour immune response to be between tumour cells, antigen presenting cells and T-cells, which are split into two sub-types, helper and cytotoxic. Their interactions, summarised in Fig. 1, are governed by the following reactions:

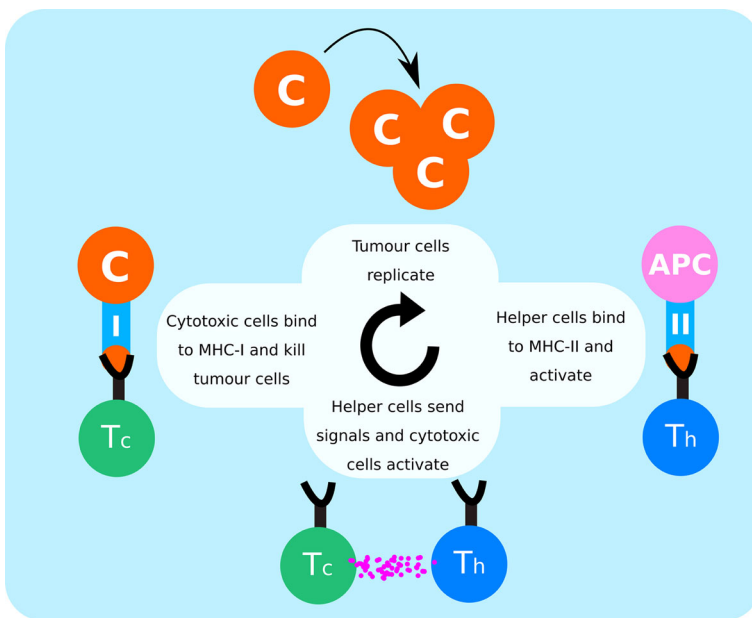


Fig. 1 Summary of cellular interactions between tumour cells (C), antigen presenting cells (APCs), helper T cells (Th) and cytotoxic T cells (Tc) in the anti-tumour immune response

- Tumour cells, C , replicate at a constant rate r and produce free floating antigens that are detected by the immune system,

$$C \xrightarrow{r} 2C. \tag{1}$$

- Tumour cells compete for resources such that there is a maximum concentration of tumour cells, ρ_c , in a finite volume

$$C + C \xrightarrow{r/\rho_c} C. \tag{2}$$

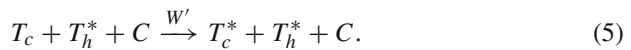
- Professional antigen presenting cells, B , such as dendritic cells, take up free floating antigens, process them into peptides, and display them on surface molecules MHC-II, P ,



- Helper T-cells, T_h , bind to the peptide-MHC-II complex and activate, T_h^* ,



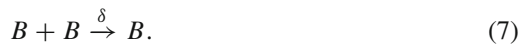
- Cytotoxic T-cells, T_c , are activated, T_c^* , by both cytokines from activated helpers and stimulation from tumour cells that the cytotoxic T-cells are specific to,



- Activated helpers induce the proliferation of antigen presenting cells



- Professional antigen presenting cells maintain homeostasis and are assumed to compete at rate δ for the same resources,



- Activated cytotoxic T-cells eliminate tumour cells after docking to MHC-I,



The ‘killing’ rate, κ , is proportional to the rate at which cytotoxic cells bind and induce cytotoxic death, k , and the expression of MHC-I, γ , which can decrease throughout the development of the tumour. This is such that $\kappa = k\gamma$. For the remainder of this paper we set $k = 1$ and, without loss of generality, focus on the expression of MHC-I, $\gamma \in [0, 1]$, with $\gamma = 0$ corresponding to no tumour cells

expressing MHC-I and $\gamma = 1$ corresponding to maximum MHC-I expression in the tumour. In principle, γ will vary with time, but to simplify the analysis we assume for now that it is constant and comment later on the effect of time-dependent γ .

2.2 A statistical mechanics description of the immune system

We consider a solid tumour to occupy a space of fixed volume V . This volume is comprised of cells including helper and cytotoxic T-cells, professional antigen presenting cells and tumour cells. We represent the number of tumour cells, antigen presenting cells, and antigen presenting cells with MHC-II peptide complex, by the variables $[C]$, $[B]$ and $[P]$, respectively. The concentration of each of these cells is then simply given by their number over the volume of the solid tumour, $c = [C]/V$, $b = [B]/V$ and $p = [P]/V$. The volume is permeable such that T-cells can move freely from the periphery into the solid tumour. We consider there to be a large population of T-cells, each labelled by an index $i = 1, \dots, N$, such that the density of T-cells, $\rho = N/V$, is finite. T-cells can be divided in two sub-types: helper and cytotoxic. We describe the sub-type of each T-cell i by a binary variable η_i ,

$$\eta_i = \begin{cases} 1, & \text{if T-cell } i \text{ is a helper T-cell} \\ 0, & \text{if T-cell } i \text{ is a cytotoxic T-cell} \end{cases} \quad (9)$$

that we regard as random, with distribution

$$P(\eta) = \epsilon \delta_{\eta,1} + (1 - \epsilon) \delta_{\eta,0} \quad (10)$$

where the parameter $\epsilon \in [0, 1]$ controls the proportion of helper and cytotoxic T-cells, such that if $\epsilon = 0$ all T-cells are cytotoxic, while if $\epsilon = 1$ all T-cells are helpers. The helper/cytotoxic ratio is given by $R = \epsilon/(1 - \epsilon)$.

Each T-cell has receptors known as T-cell receptors (TCRs). A given TCR is specific to an antigen, and if they are not specific to tumour associated antigens, they will not form part of the immune response. To model this we introduce a binary random variable ξ_i

$$\xi_i = \begin{cases} 1, & \text{if T-cell } i \text{ can bind to a cancer cell} \\ 0, & \text{otherwise} \end{cases} \quad (11)$$

drawn from the distribution

$$P(\xi|\eta) = [A_\eta \delta_{\xi,1} + (1 - A_\eta) \delta_{\xi,0}] \quad (12)$$

such that $A_\eta \in [0, 1]$ controls the fraction of T-cells of type η that are specific to tumour associated antigens. In general there may be differences in the size of the helper and cytotoxic pools of T-cells that are specific to tumour antigens, however, in the lack of detailed knowledge about such differences, we assume statistical independence of η and ξ such that $A_\eta = A \forall \eta = 0, 1$.

As explained in Sect. 2.1, T-cells can be found in two states, active and inactive. Since the activation of T-cells evolves with time over the course of the immune response, each T-cell can be described by a time-dependent state variable $\sigma_i(t)$ where,

$$\sigma_i(t) = \begin{cases} 1, & \text{if T-cell } i \text{ is activated at time } t \\ 0, & \text{otherwise.} \end{cases} \quad (13)$$

During the immune response, T-cell activation occurs through a TCR-dependent pathway whereby the TCR binds to the peptide complex of MHC molecules and a condition is met such that the T-cell activates. The precise nature of the activation of T-cells is debated, but there is evidence to suggest that sufficient binding time is required for activation (Allard et al. 2017; Tian et al. 2007; Robert et al. 2012; Tkach and Altan-Bonnet 2013; Aleksic et al. 2010). Due to noise, inherent in biological systems, T-cells are likely to bind and unbind in a stochastic manner, therefore we treat T-cell activation as a stochastic process, following previous studies of T-cell activation in the literature (Wedagedera and Burroughs 2006; Lipniacki et al. 2008; Agliari et al. 2013; Annibale et al. 2018).

For simplicity, we assume that T-cells update their activation state at regular time intervals of duration Δ (which will eventually be sent to zero to retrieve continuous time dynamics), according to the rule

$$\sigma_i(t + \Delta) = \theta \left(\eta_i \xi_i p(t) + (1 - \eta_i) \xi_i c(t) \frac{1}{V} \sum_{j=1}^N \sigma_j(t) \eta_j \xi_j - \phi(t) - T z_i(t) \right), \quad (14)$$

where $\theta(x) = 1$ for $x > 0$ and 0 otherwise, and $z_i(t)$ is a zero-averaged random variable with suitably normalised variance mimicking fast noise in the biological environment or stochasticity in T-cell activation. The parameter T controls the noise level, such that the activation dynamics is fully stochastic for $T \rightarrow \infty$ and it is deterministic for $T = 0$. In the absence of noise ($T = 0$), Eq. (14) states that a T-cell i will activate if it receives a strong enough activation signal from the environment, i.e. if the activation signal is above a certain threshold $\phi(t)$. The activation signal depends on the nature of the T-cell, helper or cytotoxic, and it is given by the first and second term in the round brackets, respectively. A helper T-cell i (i.e. $\eta_i = 1$) will activate if it is specific to tumour antigens (i.e. $\xi_i = 1$) and there is a sufficient concentration $p(t)$ of antigen presenting cells with tumour associated antigens, while a cytotoxic T-cell ($\eta_i = 0$) will activate if it is specific to tumour antigens (i.e. $\xi_i = 1$) and it is sufficiently co-stimulated by tumour cells and active, tumour specific helpers, whose concentrations are $c(t)$ and $V^{-1} \sum_{j=1}^N \sigma_j(t) \eta_j \xi_j$, respectively. The threshold $\phi(t)$ mimicks any barrier that T-cells need to overcome to activate, including immunosuppressive effects due to T-cell exhaustion and inactivation via Treg cells. Noise (i.e. $T > 0$) can be interpreted as the amount that T-cells deviate from their deterministic activation rules. In addition to the binding and unbinding of T-cells to MHC molecules, noise may also account for alternative activation pathways. For

example, cytotoxic T-cells may not necessarily need helper T-cells to activate, they can be directly activated by APCs.

We note that Eq. (14) models reactions (4) and (5) in the presence of noise, at the *microscopic* level of individual T-cells. Alternatively, one could model (4) and (5) at population level, via reaction kinetics (i.e. ODE) equations for the densities of active and inactive T-cells, valid under the assumptions of a well-mixed system and negligible fluctuations due to discreteness of cells. Noise could be included at population level, by introducing a reaction for spontaneous activation and deactivation of T-cells, whose rates would lead to additional free parameters in the model. Our approach starts instead from stochastic equations for the microscopic cell states, which do not require the above assumptions and keep the number of free parameters to a minimum. Macroscopic cell densities, such as those involved in reaction kinetics, can be obtained within our approach, as sums of microscopic variables, e.g. the density of active T-cells that are specific to tumour antigens can be retrieved as $V^{-1} \sum_{i=1}^N \xi_i \sigma_i$.

Next, we write differential equations for the concentrations of tumour and antigen presenting cells in the local environment, by modelling the cellular reactions in (1)-(8) at population level. Their evolution can be written in the following way

$$\frac{dc}{dt} = \left[r - \gamma \frac{1}{V} \sum_{i=1}^N \sigma_i (1 - \eta_i) \xi_i \right] c - \frac{rc^2}{\rho_c} \quad (15)$$

$$\frac{db}{dt} = b \left(\lambda \frac{1}{V} \sum_{i=1}^N \sigma_i \eta_i \xi_i - \delta b \right) \quad (16)$$

$$\frac{dp}{dt} = \pi^+ bc - \pi^- p. \quad (17)$$

We see here that the dependence on T-cell activation, described by the stochastic variable $\sigma_i(t)$, means that the concentrations c , b and p are also subject to stochastic fluctuations.

Equation (15) contains three terms describing the change in tumour cell concentration with time, $\frac{dc}{dt}$. The first term states that c will increase at a rate r proportionally with c , corresponding to Eq. (1). The second term describes the effect of the T-cells on the tumour cells as in Eq. (8): a sum is taken over all the T-cells, and a non-zero contribution is only made by T-cells which are cytotoxic, specific to tumour cells and active, i.e. when $\sigma_i = 1 - \eta_i = \xi_i = 1$. Therefore, the second term states that tumour cells will be killed at a rate $\kappa = \gamma$ and proportionally with the concentration of tumour cells and the fraction of active, specific cytotoxic T-cells. Finally, the third term states that in the absence of the second term, i.e the T-cell response, the tumour cells will reach a carrying capacity concentration ρ_c , as described in Eq. (2).

The equation for $\frac{db}{dt}$ can similarly be annotated. The first term states that antigen presenting cells will proliferate due to the presence of active helper T-cells at rate λ , as in Eq. (6). The second term describes competition at constant rate δ , as described in Eq. (7). The first and second terms in $\frac{dp}{dt}$ correspond to the reactions described in (3) and account for the antigen uptake and presentation by antigen presenting cells at rate π^+ , and the reverse process where a receptor is freed for the uptake of new antigen,

at rate π^- , respectively. In principle, Eq. (16) should contain a term reflecting the loss of naive APCs becoming activated APCs, $-\frac{1}{n}\pi^+bc$, and a gain term reflecting the reverse process $+\frac{1}{n}\pi^-p$. Here n represents the number of antigens that APCs can process at one time. Since APCs, such as dendritic cells, can process multiple antigens via a multitude of pathways and receptors (Platt et al. 2010) and a large number of antigen receptors $\mathcal{O}(10^5)$ is also present on B cells (Li et al. 2019), we consider n to be large, such that terms $\mathcal{O}(1/n)$ can be neglected. We note that these terms will vanish anyway in the steady state, the main focus of our study, by Eq. (17).

3 Results

3.1 Macroscopic dynamics of T-cell activation

From a set of cellular reactions we have started to build a set of differential equations, with the inclusion of a microscopic description of T-cells. As they stand we can not solve Eqs. (15)–(17) directly, due to the dependence on the stochastic variables $\sigma_i(t)$. To make analytical progress we define the macroscopic observables,

$$m(\sigma) = \frac{1}{V} \sum_{i=1}^N \sigma_i \eta_i \xi_i \tag{18}$$

$$a(\sigma) = \frac{1}{V} \sum_{i=1}^N \sigma_i \xi_i. \tag{19}$$

where $\sigma \in \{0, 1\}^N$, representing the density of active, specific helpers and the density of active, specific T-cells, respectively. With these definitions Eqs. (15)–(17) can be written as follows,

$$\begin{aligned} \frac{dc}{dt} &= \left[r - \gamma (a(\sigma) - m(\sigma)) - \frac{rc}{\rho c} \right] c \\ \frac{db}{dt} &= b (\lambda m(\sigma) - \delta b) \\ \frac{dp}{dt} &= \pi^+ bc - \pi^- p. \end{aligned} \tag{20}$$

We now seek to derive the time evolution of the macroscopic observables $a(\sigma)$ and $m(\sigma)$. To this purpose, we must specify the statistical properties of the activation noise. Information about the latter is very scarce in biological literature (Irvine et al. 2002; Wedagedera and Burroughs 2006; Burroughs and Van Der Merwe 2007). A natural choice would be to assume a Gaussian distribution of noise however, for convenience of analysis and without loss of generality, we consider a distribution of noise more common in statistical physics (see Appendix for details).

Assuming that T-cells are updated sequentially, Eq. (14) can be cast into a master equation for the time-dependent probability $P_t(\sigma)$, by setting $\Delta = 1/N$ in Eq. (14),

and taking the limit $N \rightarrow \infty$ (Coolen and Ruijgrok 1988). This is detailed in the Appendix where equations for the time evolution of the macroscopic observables $a(\sigma)$ and $m(\sigma)$ are also derived. It will turn out that fluctuations of these quantities around their averages, $m(t) = \sum_{\sigma} P_t(\sigma)m(\sigma)$ and $a(t) = \sum_{\sigma} P_t(\sigma)a(\sigma)$, vanish as the number of T-cells, N , is sent to infinity and that the evolution of these averages is governed by the equations

$$\begin{aligned} \frac{dm}{dt} &= -m + \frac{\rho}{2} \left\langle \eta \xi \left[1 + \tanh \left(\frac{\beta}{2} (\eta \xi p + (1 - \eta) \xi cm - \phi(t)) \right) \right] \right\rangle_{\eta, \xi} \\ \frac{da}{dt} &= -a + \frac{\rho}{2} \left\langle \xi \left[1 + \tanh \left(\frac{\beta}{2} (\eta \xi p + (1 - \eta) \xi cm - \phi(t)) \right) \right] \right\rangle_{\eta, \xi}. \end{aligned} \tag{21}$$

In the above the density of T-cells $\rho = \frac{N}{V}$ is assumed to be finite when $N \rightarrow \infty$ and $\langle \dots \rangle_{\eta, \xi}$ denotes the average over the joint distribution,

$$P(\eta, \xi) = \lim_{N \rightarrow \infty} \frac{1}{N} \sum_i \delta_{\eta, \eta_i} \delta_{\xi, \xi_i}. \tag{22}$$

As stated earlier, we assume that $P(\eta, \xi) = P(\eta)P(\xi)$, i.e. the probability of a T-cell having a conjugate receptor to the tumour associated antigens is not dependent on whether T-cell i is helper or cytotoxic. Equations (10) and (12) may then be used to compute the averages in (21).

Finally, we take Eqs. (20) and replace $m(\sigma)$ and $a(\sigma)$ with their thermodynamic averages m and a , which is equivalent to a mean-field approximation, that we show in the appendix to be exact in the limit $N \rightarrow \infty$. This allows us to get a small, closed system of ODEs,

$$\begin{aligned} \frac{dc}{dt} &= \left[r - \gamma(a - m) - \frac{rc}{\rho c} \right] c \\ \frac{db}{dt} &= b(\lambda m - \delta b) \\ \frac{dp}{dt} &= \pi^+ bc - \pi^- p \\ \frac{dm}{dt} &= -m + \frac{\epsilon A \rho}{2} \left[1 + \tanh \left(\frac{\beta}{2} (p - \phi(t)) \right) \right] \\ \frac{da}{dt} &= -a + \frac{A \rho}{2} \left[1 + \epsilon \tanh \left(\frac{\beta}{2} (p - \phi(t)) \right) + (1 - \epsilon) \tanh \left(\frac{\beta}{2} (cm - \phi(t)) \right) \right]. \end{aligned} \tag{23}$$

By describing the T-cell dependent anti-tumour immune response with ODEs we have neglected the role of spatial heterogeneity in the evolution of tumours. This was done in the spirit of capturing the interplay between the CD4⁺/CD8⁺ T-cell ratio and MHC-I expression with a simple model, amenable to analytical solution. In principle one could model spatial heterogeneity in the T-cell dependent immune response by

making the variables ϵ and A functions of spatial position. This would result in c , b and p becoming spatially-dependent. However, further considerations would need to be made to account for cellular drift in space. By neglecting spatial dependencies, our approach is equivalent to modelling a small, macroscopic region of a solid tumour where spatially-dependent variables can be regarded as uniform.

3.2 Conditions for tumour eradication

We use the system of Eqs. (23) to derive a set of conditions which will qualitatively describe how the anti-tumour immune response changes with parameters of the model. First, we write the system of equations in a more compact way by defining the vector $\mathbf{x} = (c, b, p, m, a)$ such that $\dot{\mathbf{x}} = \mathbf{F}(\mathbf{x})$, where each component of the vector \mathbf{F} is the RHS of the corresponding ODE. Second, we find fixed points of the dynamics from $\dot{\mathbf{x}} = \mathbf{0}$ and analyse their stability by inspecting the eigenvalues of the Jacobian $\partial\mathbf{F}/\partial\mathbf{x}$. The system will allow for fixed points if the activation threshold $\phi(t)$, accounting for immunosuppressive effects, is stationary. In the remainder of this work, we will focus on a vanishing stationary threshold $\phi(t) = 0 \forall t$. In this case our model will provide a lower limit on the size of the tumour, as immunosuppressive signals reduce the anti-tumour immune response. We find that there are two fixed points which, subject to some condition, are stable. There are two other fixed points but they are always unstable. The potentially stable fixed points are given by,

$$\mathbf{x}_1 = (0, \frac{\lambda m^*}{\delta}, 0, m^*, a^*), \tag{24}$$

where $m^* = \frac{\epsilon A \rho}{2}$ and $a^* = \frac{A \rho}{2}$ and

$$\mathbf{x}_2 = (c^*, \frac{\lambda m^*}{\delta}, \frac{\pi + \lambda}{\pi - \delta} c^* m^*, m^*, a^*) \tag{25}$$

where c^* , m^* and a^* are the solution to the system of equations

$$c^* = \frac{\rho_c(r - \gamma(a^* - m^*))}{r} \tag{26}$$

$$m^* = \frac{\epsilon A \rho}{2} \left(1 + \tanh \left(\frac{\beta \pi + \lambda}{2\pi - \delta} c^* m^* \right) \right) \tag{27}$$

$$a^* = \frac{A \rho}{2} \left(1 + \epsilon \tanh \left(\frac{\beta \pi + \lambda}{2\pi - \delta} c^* m^* \right) + (1 - \epsilon) \tanh \left(\frac{\beta}{2} c^* m^* \right) \right). \tag{28}$$

The fixed point \mathbf{x}_1 corresponds to tumour eradication, $c^* = 0$, whereas \mathbf{x}_2 corresponds to tumour escape, $c^* \neq 0$. The size of the tumour at \mathbf{x}_2 varies with the parameters of the system. When T-cells are all cytotoxic, $\epsilon = 0$, there is no signal from helper cells $m^* = 0$, and all T-cell signal comes from cytotoxic cells, $a^* = \frac{A \rho}{2}$, resulting in a tumour below the carrying capacity, $c^* = \rho_c \left(1 - \frac{\gamma A \rho}{2} \right)$. However, when all T-cells are helpers, $\epsilon = 1$, we have that the net T-cell signal is equivalent to the helper T-cell

signal, $m^* = a^*$, and that the tumour reaches the carrying capacity, $c^* = \rho_c$. From analysis of the eigenvalues of the Jacobian $\partial \mathbf{F} / \partial \mathbf{x}$ we find that \mathbf{x}_1 is stable when,

$$\gamma > \gamma_c = \frac{2r}{A\rho}(1 + R) \tag{29}$$

when this condition is not met \mathbf{x}_1 is unstable. To assess the stability of \mathbf{x}_2 we should analyse the eigenvalues of the Jacobian evaluated at \mathbf{x}_2 , however the eigenvalues are found to be non-trivial and a condition for stability based on a single parameter as in (29) is not tractable.

To make progress analytically, we look at the long-time dynamics of the model. To this end, we separate three different timescales of immune response dynamics: the timescale of tumour cell division τ_c , antigen presentation τ_p , and T-cell activation τ_a . To do so, we re-scale processes with timescale τ such that $t \rightarrow \frac{t}{\tau}$. After this re-scaling our system of equations in (23) becomes,

$$\begin{aligned} \tau_c \frac{dc}{dt} &= \left[r - \gamma(a - m) - \frac{rc}{\rho_c} \right] c \\ \tau_p \frac{db}{dt} &= b(\lambda m - \delta b) \\ \tau_p \frac{dp}{dt} &= \pi^+ bc - \pi^- p \\ \tau_a \frac{dm}{dt} &= -m + \frac{\epsilon A\rho}{2} \left[1 + \tanh\left(\frac{\beta}{2} p\right) \right] \\ \tau_a \frac{da}{dt} &= -a + \frac{A\rho}{2} \left[1 + \epsilon \tanh\left(\frac{\beta}{2} p\right) + (1 - \epsilon) \tanh\left(\frac{\beta}{2} cm\right) \right]. \end{aligned} \tag{30}$$

To study the long time dynamics the relative magnitude of these timescales must be specified. We assume that $\tau_p \rightarrow 0$ such that the processing and presentation of antigens is fast implying that the variables changing at this timescale will approach their stable nullcline, $b = \frac{\lambda m}{\delta}$ and $p = \frac{\pi^+ \lambda m c}{\pi^- \delta}$. Then there are two options: either tumour cell division is a faster process than T-cell activation or vice versa. If we consider the case that T-cell activation is faster than tumour cell division, i.e $\tau_a \ll \tau_c$, then we can formally send $\tau_a \rightarrow 0$ and find that the T-cell activation variables approach their nullclines,

$$\begin{aligned} a &= \frac{A\rho}{2} \left[1 + \epsilon \tanh\left(\frac{\beta}{2} p\right) + (1 - \epsilon) \tanh\left(\frac{\beta}{2} cm\right) \right] \\ m &= F^{-1}(c) \end{aligned}$$

where

$$F(m) = \frac{2\pi^- \delta}{\beta \pi^+ \lambda m} \tanh^{-1} \left(\frac{2m}{\epsilon A\rho} - 1 \right). \tag{31}$$

This reduces the system (30) to a single ODE,

$$\frac{dc}{dt} = \left[r - \frac{\gamma A \rho}{2} (1 - \epsilon) \left[1 + \tanh \left(\beta c F^{-1}(c)/2 \right) \right] - \frac{rc}{\rho_c} \right] c = f(c) \tag{32}$$

which has two fixed points given by

$$c^* = 0 \tag{33}$$

$$c^* = \rho_c \left(1 - \frac{\gamma A \rho}{2r} (1 - \epsilon) \left[1 + \tanh \left(\beta c^* F^{-1}(c^*)/2 \right) \right] \right) \tag{34}$$

corresponding, respectively, to tumour eradication and large stable tumour formation. The non-trivial fixed point, $c^* > 0$, can be found using the relation $F^{-1}(c^*) = m^*$ via the numerical solution of (26)-(28).

To inspect the stability of the fixed points we evaluate the derivative $f'(c)$ of the ‘velocity’ function defined in (32). The fixed point $c^* = 0$ is stable when $f'(0) < 0$ giving us the condition $\gamma > \gamma_c = \frac{2r}{A\rho} \frac{1}{1-\epsilon}$ which is equivalent to (29). The non-trivial fixed point $c^* > 0$ will be stable when $f'(c^*) < 0$, yielding

$$\gamma < \gamma^* = \frac{2r}{A\rho} (1 + R) \left\{ 1 - \frac{\beta}{2} c^* \left[m^* + \frac{c^*}{F'(m^*)} \right] \cosh^{-2} (\beta c^* m^*/2) \right\}^{-1}. \tag{35}$$

Since it is not necessary that $\gamma_c = \gamma^*$, there is a possibility that either (i) $\gamma^* < \gamma < \gamma_c$ and both fixed points are unstable or (ii) $\gamma_c < \gamma < \gamma^*$ and both fixed points are stable; this would suggest that the dynamics are non-trivial and can not be analysed through linear stability analysis alone. To investigate which, if any, of the two scenarios is taking place, we perform limiting analysis of the stability condition. We first note that for meaningful values of m i.e $0 < m < \epsilon A \rho$ which must be, by definition, at most of order $\mathcal{O}(1)$, we can show that $F'(m) > 0$. The term $\frac{\beta}{2} c^* \left[m^* + \frac{c^*}{F'(m^*)} \right] \cosh^{-2} (\beta c^* m^*/2) \sim \mathcal{O}(\frac{c^{*2}}{\exp(c^*)}) < 1$ which vanishes at both $c^* \rightarrow 0$ and $c^* \rightarrow \infty$. It then follows from Eqs. (34) and (35) that,

$$\text{as } \gamma \rightarrow 0^+, c^* \rightarrow \rho_c^- \implies \gamma^* \geq \gamma_c^+ \tag{36}$$

with equality at $\rho_c \rightarrow \infty$. We can also look at the limit that the γ approaches its critical value to find,

$$\text{as } \gamma \rightarrow \gamma_c^-, c^* \rightarrow 0^+ \text{ and } \gamma^* \rightarrow \gamma_c^+. \tag{37}$$

However, the exact value of γ^* can only be found through numerical solution of Eqs. (26) and (27). Solving the latter, see Fig. 2 (left panel), we find that

$$\gamma > \gamma_c \implies \gamma > \gamma^* \tag{38}$$

$$\gamma < \gamma_c \implies \gamma < \gamma^* \tag{39}$$

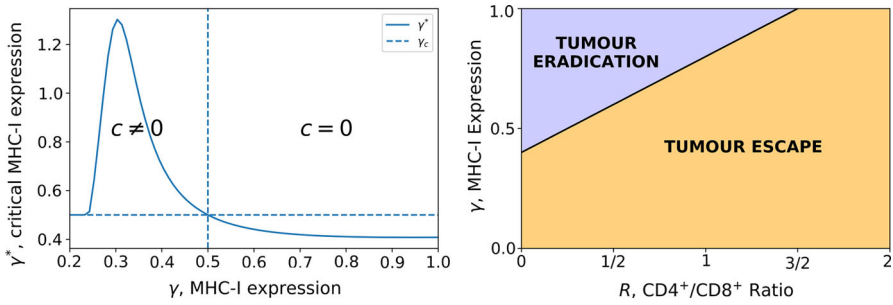


Fig. 2 Left: The fixed point of Eq. (32) where $c \neq 0$ is stable when $\gamma < \gamma^*$. We solve Eq. (34) numerically to plot γ^* as a function of γ . When $\gamma > \gamma_c$ the fixed point where $c = 0$ is stable. The value of γ_c is indicated by the dashed lines. The model parameters used are: tumour replication rate $r = 0.15$, CD4/CD8 ratio $R = 1/3$, and specific T-cell density $A\rho = 0.8$. All other parameters are set to 1. Right: γ_c is plotted against the helper/cytotoxic ratio R . Tumour cells are removed above the critical line. The model parameters used are: tumour replication rate $r = 0.2$, specificity of T-cells $A = 1$ and density of T-cells $\rho = 1.0$

which implies that the fixed points exchange stability as $\gamma \rightarrow \gamma_c$.

From the analysis of the long time dynamics of the system (30), and by taking into account different timescales of processes, we have shown that there are two fixed points where $c = 0$ or $c = c^*$. If the MHC-I expression is above some critical value, $\gamma > \gamma_c$, the fixed point $c = 0$ is stable and $c = c^*$ is unstable, whereas the reverse is true if $\gamma < \gamma_c$. In doing so we have assumed that $\tau_a \ll \tau_c$. If we assume the reverse, $\tau_c \ll \tau_a$, we find that the system has the same fixed points with identical stability criteria. This implies that the long-time dynamics will be the same, although transient behaviour will differ.

This shows that there is a critical value of MHC-I expression, above which the tumour will be eradicated, and below which it will reach some stable tumour size. Furthermore, the critical value of MHC-I depends linearly through the helper/cytotoxic ratio R . To remove tumour cells a large population of cytotoxic T-cells is required and this depends on the expression of MHC-I. This is illustrated in Fig. 2 (right panel). This implies that measuring CD4⁺/CD8⁺ alone may yield incorrect understanding of tumour progression *in vivo* since it also depends on the expression of MHC-I. With a low MHC-I expression, a CD4⁺/CD8⁺ ratio that would have been considered healthy for high MHC-I expression would not lead to complete tumour eradication. We note that this figure shows that higher CD8 and higher MHC-I are associated with lower tumour size, consistent with current data (Turcotte et al. 2014).

The stability of the fixed points does not depend on the T-cell activation noise level, $\beta^{-1} = T$. The noise does however affect the size of the escaped tumour as shown in Fig. 3, obtained by solving together Eqs. (26) and (27) numerically. An additional observation is the dependence of γ_c on the parameters A and ρ in (29). These parameters, respectively, represent the specificity and infiltration of T-cells in the tumour, and their relationship with γ_c suggests that small changes in the infiltration of T-cells can greatly affect tumour growth.

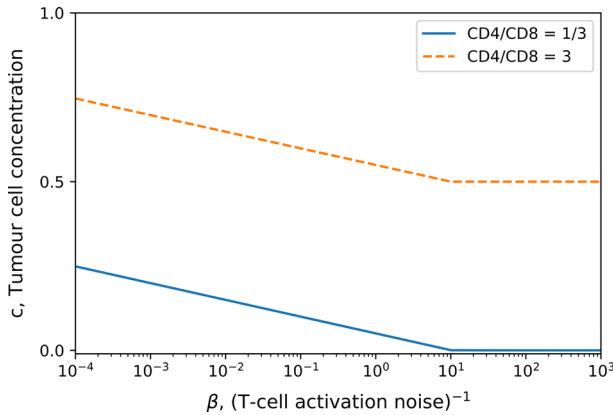


Fig. 3 Equilibrium tumour concentration plotted as a function of inverse T-cell activation noise β . Activation noise is increasing from right to left. The tumour replication rate is $r = 0.5$, the carrying capacity concentration is $\rho_c = 1000$, and the MHC-I expression and specific tumour density are set to $\gamma = A = \rho = 1$. The tumour cell concentration is normalised with respect to the carrying capacity ρ_c

3.3 Tumour size with immune parameters

This model provides predictions for the dependence of the size of the tumour, given by Eqs. (26) and (27), on different immune parameters. Figure 4 shows how the size of the tumour varies with MHC-I expression (left panel) and infiltration of specific T-cells $A\rho$ (right panel) and it shows that it increases when the ratio $CD4^+/CD8^+$ is larger. For a high $CD4^+/CD8^+$ we see a discontinuity in the stable tumour size. This is due to the figure showing the tumour size dynamically reached at equilibrium. Above the critical value of infiltration, which can also be found from (29), there are enough T-cells to remove tumour cells, but below this value the tumour can grow to a stable size that depends on all other parameters of the system.

A common problem with ODE models of immunology is that they require temporal data for validation - which can be hard to come by for both practical and ethical reasons. Our model is based upon immune dynamics but can be used to produce predictions not based on time as in the case with the figures discussed in this section. Concurrent measurements of MHC-I, T-cell infiltration and $CD4^+/CD8^+$ are lacking in the literature, but are examples of data which could be used to validate this model.

3.4 Optimal helper/cytotoxic ratio

Another feature of this model is the ability to predict an optimal helper/cytotoxic ratio R . Here we define optimal to mean yielding the lowest stable tumour size when Eq. (32) equilibrates to the fixed point $c = c^*$. We parameterised the system such that the fixed point $c = c^*$ was always stable and considered the numerical solution for the stable tumour cell concentration, (26)-(28), for different values of R as shown in Fig. 5. As the cytotoxic T-cell pool decreases the tumour cell concentration increases, as expected. However, if there are not enough helper cells to activate the cytotoxic

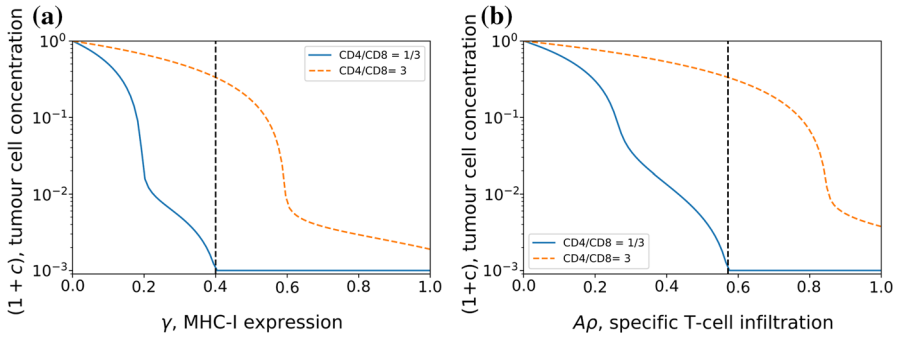


Fig. 4 Equilibrium concentration of tumour cells plotted as a function of MHC-I expression in (a) and as a function of specific tumour T-cell infiltration in (b), displayed for two different helper/cytotoxic T-cell ratios. Here the tumour replication rate is $r = 0.15$, the activation noise is $\beta^{-1} = 1$, T-cell density is $\rho = 1$, the specificity in (a) is set to $A = 1$, the MHC-I expression in (b) is $\gamma = 0.7$, and the carrying capacity is set to $\rho_c = 1000$. The tumour cell concentration has been normalised by the carrying capacity ρ_c . For the case of $CD4^+/CD8^+ = 1/3$ the dynamically reached equilibrium tumour cell concentration, given by Eqs. (33) and (34), is plotted to the right and the left of the dashed (vertical) lines respectively

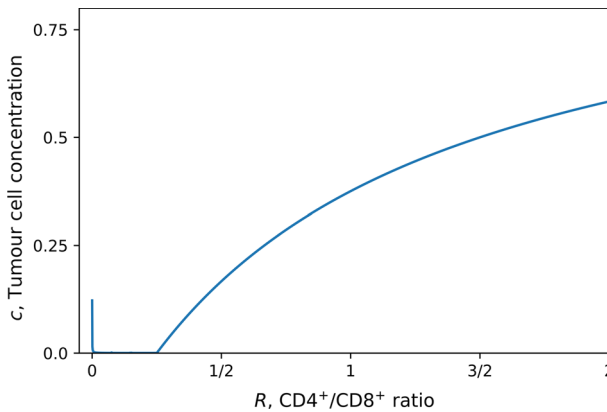


Fig. 5 Cell concentration of a tumour which has escaped plotted as a function of the helper/cytotoxic T-cell ratio R for $\beta = 100$, $r = 0.8$, $A = \gamma = \rho = 1$, $\rho_c = 1000$. The tumour cell concentration has been normalised with the carrying capacity ρ_c

population, the tumour reaches a large size, corresponding to the peak around $R = 0$. Note that even in absence of helper T-cells, cytotoxic T-cells may still activate at finite noise levels (corresponding to activation via pathways independent of helper cells.) This explains why at $R = 0$ the tumour cell concentration is still below the carrying capacity ρ_c in Fig. 5. An interesting feature of this model is that it shows that there is a range of values of R for which the tumour size is relatively small. This suggests that the immune system is robust to changes in the $CD4^+/CD8^+$ ratio. This is encouraging as the function of the immune system should not be sensitive to changes in this ratio.

3.5 Time variation of MHC-I expression

In our model we have treated the expression of MHC-I, γ , as a constant, however in principle it should evolve with time, $\gamma = \gamma(t)$. As the tumour progresses, tumour cells with low expression of MHC-I will evade the immune response and will have an advantage over tumour cells that have high MHC-I expression. This selective pressure means that the MHC-I expression in the bulk tumour will decrease over time. Analytical progress with time dependent MHC-I expression $\gamma(t)$ is difficult, so to achieve this we reduce our system of equations by assuming *all* T-cells are active i.e $a = A\rho/2$ and $m = \epsilon A\rho/2$. By fixing a and m to their maximum physical values, the system of equations reduces to a single equation for the tumour cell concentration,

$$\frac{dc}{dt} = \left[r - \bar{A}\gamma(t) - \frac{rc}{\rho_c} \right] c, \quad (40)$$

with

$$\bar{A} = \frac{A\rho(1-\epsilon)}{2}. \quad (41)$$

We refer to this limit as a “best-case” scenario, since if a and m are allowed to vary below their maximum value, the tumour concentration will be higher than if locked at their maximum value. The solution of the above equation, given by

$$c(t) = \frac{c_0\rho e^{\int_0^t (r-\bar{A}\gamma(s))ds}}{\rho_c + c_0 \int_0^t e^{\int_0^s (r-\bar{A}\gamma(s'))ds'} ds}, \quad (42)$$

requires knowledge of $\gamma(t)$. The latter has not been studied in the literature, however, we can bound the solution for a family of $\gamma(t)$ functions if we assume that the maximum, γ_{\max} , and minimum, γ_{\min} , values of the function are known. We find the upper bound to be as follows

$$c(t) \leq \frac{c_0\rho_c e^{t(r-\bar{A}\gamma_{\min})}}{\rho_c + \frac{c_0}{r-\bar{A}\gamma_{\max}} \left(e^{t(r-\bar{A}\gamma_{\max})} - 1 \right)}. \quad (43)$$

The long-time behaviour of the upper bound in the above depends on γ_{\min} as follows

$$c(\infty) \leq \begin{cases} 0, & \text{if } \gamma_{\min} > \frac{r}{\bar{A}} = \gamma_c \\ \infty & \text{otherwise,} \end{cases} \quad (44)$$

where we have recovered that for the tumour to be eradicated as $t \rightarrow \infty$ we require that $\gamma > \gamma_c$.

A tighter bound on $c(t)$ can be found with a specific form of $\gamma(t)$. In particular, if we assume that the expression of MHC-I decays exponentially,

$$\gamma(t) = e^{-\frac{t}{\tau_\gamma}} \tag{45}$$

where τ_γ is the timescale of MHC-I decay, the solution can be bound as follows,

$$\frac{c_0 \rho_c e^{\bar{A}\tau_\gamma \left(e^{-\frac{t}{\tau_\gamma}} - 1 \right)}}{\rho_c e^{-rt} + c_0 (1 - e^{-rt})} \leq c(t) \leq \frac{c_0 \rho_c e^{\bar{A}\tau_\gamma} e^{-\frac{t}{\tau_\gamma}}}{\rho_c e^{-rt + \bar{A}\tau_\gamma} + c_0 (1 - e^{-rt})} \tag{46}$$

where in the above we have used $\int_0^t e^{rs} ds \leq \int_0^t e^{rs + \tau_\gamma \bar{A} e^{-\frac{s}{\tau_\gamma}}} ds \leq \int_0^t e^{rs + \tau_\gamma \bar{A}} ds$. If we now consider the long-time behaviour of $c(t)$ we find that

$$\rho_c e^{-\bar{A}\tau_\gamma} \leq c(\infty) \leq \rho_c. \tag{47}$$

The upper bound is now finite in the long time limit, and is equal to the carrying capacity concentration, as would be expected. We see that the lower bound of $c(t)$ is also finite. The latter is due to $\gamma_{\min} < \gamma_c$. Therefore, according to this model the exponential decay of MHC-I prohibits the eradication of tumours. However, it is important to stress that if the decay rate is sufficiently slow, the tumour cell concentration can become very small. All calculations have been made under the assumption that $\rho = \frac{N}{V} = \mathcal{O}(1)$. We show in the appendix that in this regime stochastic fluctuations are suppressed as $V \rightarrow \infty$. However, for finite N , fluctuations become of the same order as the mean, and can remove a small number of tumour cells in a finite time. Additionally, as discussed in the introduction, we neglect the role of NK cells to focus on the T-cell dependent response. However, at low MHC-I the NK cells play a more dominant role, adding an additional deleterious effect upon tumour growth.

In addition to exponential decay we have also considered a sigmoidal decay by defining

$$\gamma(t) = \frac{1}{1 + \left(\frac{t}{\tau_\gamma} \right)^g}, \tag{48}$$

which is sigmoidal for $g > 1$ where g is the shape parameter. Furthermore, the function approaches a step function as $g \gg 1$. Figure 6 shows that in the case where the tumour is initially growing at a rate faster than T-cell mediated death the behaviour changes significantly with the functional form of $\gamma(t)$. In the case of exponential MHC-I decay, the tumour cell concentration exponentially increases towards saturation. However, with a sigmoidal $\gamma(t)$, the tumour concentration increases and reaches a plateau then rapidly grows to saturation. No such difference is observed when the tumour is initially removed by the T-cells. We note that when the rate of T-cell mediated death is initially faster than the rate of replication, Fig. 6 exhibits the ‘‘three Es’’ of cancer immunoediting first discussed by Dunn et al. (2004): the tumour is initially

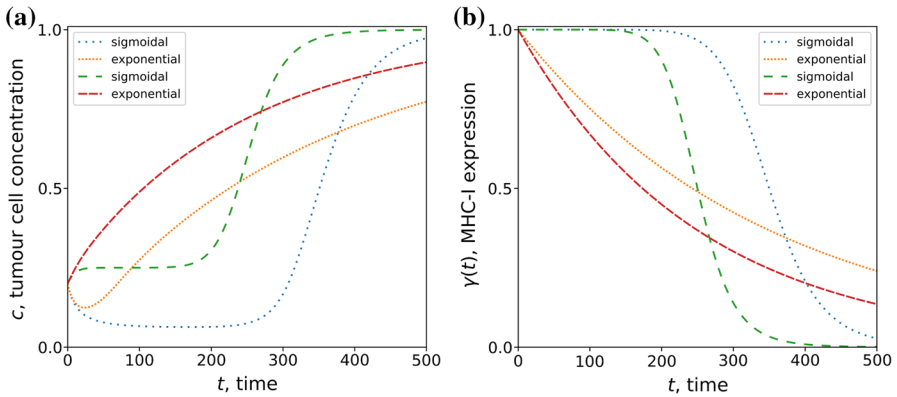


Fig. 6 Time evolution of tumour cell concentration from numerical solution of Eq. (40) (a) subject to exponential and sigmoidal MHC-I decay profiles (b). We show results for two parameterisations: tumour replication rate $r = 0.4$, timescale of MHC-I expression decay $\tau_\gamma = 350$ (dotted lines); $r = 0.5$ and $\tau_\gamma = 200$ (dashed lines). In all cases the initial tumour cell concentration is $c_0 = 20$, $\bar{A} = 0.375$, and carrying capacity concentration $\rho_c = 100$. The shape parameter for the sigmoidal decay function is $g = 10$. The tumour cell concentration has been normalised with the carrying capacity ρ_c

eliminated, reaches a period of equilibrium, and then escapes. This model suggests that the profile of $\gamma(t)$ has a dominant effect on the duration of the elimination, equilibrium and escape phases of tumour progression. A greater quantitative understanding of the loss of MHC-I in patient tumours may reveal whether MHC-I is a dominant factor in tumour equilibrium.

4 Discussion

The complexities of tumour immunology require a systemic approach to better understand cancer and inform treatment. Quantitative tools are being used to a greater extent, due to the vast data produced by next generation experimental technology; mathematical modelling being among them. Mathematical modelling can suffer from two extremes: models that include detail at the molecular level tend to focus on a small set of processes to achieve analytical results at the expense of a systemic view; on the other hand, macroscopic models which achieve greater systemic resolution, tend to have a large number of parameters, which makes statistical validation impractical, especially in absence of large data sets. In our work we used statistical mechanics and dynamical systems approaches to analyse the anti-tumour response of a simplified model of the adaptive immune system, comprising antigen presenting cells, helper T-cells and cytotoxic T-cells. The end result is a system of five ODEs that highlights the role in tumour growth of different parameters linked to key cellular processes.

Previous studies have shown that the prognostic value of the $CD4^+/CD8^+$ ratio, and the expression of MHC-I, are improved when considered in combination (Turcotte et al. 2014; Jordanova et al. 2008). Our work provides a simple model for the mechanistic interplay between these two parameters during the anti-tumour immune response,

from which apparent contradictions in the literature can be rationalised. In particular, our model suggests that, when using the CD4⁺/CD8⁺ ratio as a prognostic marker, the expression of MHC-I must also be taken into account, otherwise this may risk incorrect prognosis. A good prognosis of clinical outcome has been associated with different CD4⁺/CD8⁺ ratios across different cancers, and this model suggests that this is due to variations in MHC-I expression. If proved correct this could help to potentially unify efforts across different cancers, something that can rarely be achieved. Our model also highlights that the infiltration of specific T-cells is an important parameter, that will also affect the growth of a tumour and could potentially obfuscate the prognostic value of CD4⁺/CD8⁺ and MHC-I. Recent work has shown that the TCR repertoire of tumour infiltrating T-cells has low tumour reactivity (Scheper et al. 2019). Our model highlights the dramatic effect such a small pool of specific T-cells can have on the prognostic value of CD4⁺/CD8⁺ and MHC-I. Encouragingly, the model shows that the adaptive immune response is robust to changes in the CD4⁺/CD8⁺ ratio, as one would hope.

Our work has focused on modelling the immune response where MHC-I expression is assumed to be constant to highlight its interplay with the helper/cytotoxic ratio R . However, we have shown the role that MHC-I decay can play in the evolution of tumours. The eradication of tumours will depend on the minimum expression of MHC-I - if this is too low the T-cell response will fail and other cells, most likely NK, are required for eradication, otherwise the tumour will escape. In addition to this, our work highlights the role that the profile of MHC-I decay can have on the growth of tumours. To the best of our knowledge, there is no data measuring the time evolution of MHC-I expression in tumours to be able to estimate this profile. However, availability of such data could confirm whether the variation in MHC-I expression leads to periods of equilibrium in tumour growth.

One issue with mathematical models is that they often focus on the dynamics of immune cells, for which experimental data is rare. Although our model is based on dynamics, we have provided results which focus on non-temporal quantities that could be verified with standard measurements in immunology. We hope our model can serve as a motivation for experimental investigation into the combined effect of CD4⁺/CD8⁺ and MHC-I, and provide a useful theoretical framework to interpret results.

The work presented here is a theoretical minimal model of the adaptive immune system, and as such has limitations. For example, the model only considers the adaptive immune response and does not explicitly take into account innate immunity such as the natural killer cells and macrophages, both of which play an important role in the anti-tumour immune response. The benefit of our approach is the rigorous mathematics which can be analysed to understand qualitative behaviour, something which is often lost when considering too many parameters.

A generally applicable feature of our work is the use of non-equilibrium statistical mechanics to include an additional level of microscopic detail into the modelling of cell concentrations with ODEs. Here our model has considered the activation and sub-type of T-cells, but this framework could also be used to study other biological systems where constituent cells fluctuate stochastically between different states, while interacting with other cell concentrations in the environment. For example, there is a long history of modelling neurons as stochastic entities that fluctuate stochastically

between two states, quiescent or firing an electrical signal, (for examples see Coolen and Ruijgrok (1988); Sompolinsky et al. (1988); Nishimori et al. (1990); Coolen and Sherrington (1993)). On the other hand, neurons are known to be embedded in different tissues, including muscles and the gut, where they conceivably interact with other cells, whose concentrations may follow (approximately) deterministic dynamics.

There are two potential extensions of our work we consider to be of particular interest. Firstly, as we have discussed, our work has neglected spatial heterogeneity by modelling a small macroscopic area of a tumour which can be regarded as uniform. Spatial heterogeneity plays an important role in the anti-tumour immune response, and the extension of the techniques from non-equilibrium statistical mechanics to systems of PDEs could provide important new results although at the expense of increased model complexity. Secondly, although we consider phenotypic heterogeneity implicitly when we allow MHC-I to vary with time, we have not explicitly modelled competition between tumour cell phenotypes. This model could be extended to account for several tumour phenotypes, evolving with different rates, with heterogeneity in the T-cell response to each phenotype. Although this framework is well adapted to such a scenario, analytical progress with multiple phenotypes may provide an interesting avenue of investigation, elucidating the evolutionary game between phenotypes. Another extension would be to adapt this model to understand how tumours begin in the first place, including the healthy tissue cells from which the tumour cells derive. Tumour immunology is rich with complexity and using refined tools from statistical mechanics may shed light on this complex system of processes.

Acknowledgements All authors would like to thank Franca Fraternali and Joseph CF Ng for useful discussions regarding the direction of this work.

Funding: CJH is supported by the EPSRC Centre for Doctoral Training in Cross-Disciplinary Approaches to Non-Equilibrium Systems (CANES, EP/L015854/1).

Declarations

Conflicts of interest: All authors declare that they have no conflict of interest.

Ethics approval: N/A.

Consent to participate: N/A.

Consent for publication: N/A.

Availability of data and material: N/A.

Code availability: code is available upon request.

Open Access This article is licensed under a Creative Commons Attribution 4.0 International License, which permits use, sharing, adaptation, distribution and reproduction in any medium or format, as long as you give appropriate credit to the original author(s) and the source, provide a link to the Creative Commons licence, and indicate if changes were made. The images or other third party material in this article are included in the article's Creative Commons licence, unless indicated otherwise in a credit line to the material. If material is not included in the article's Creative Commons licence and your intended use is not permitted

by statutory regulation or exceeds the permitted use, you will need to obtain permission directly from the copyright holder. To view a copy of this licence, visit <http://creativecommons.org/licenses/by/4.0/>.

A Kramers–Moyal expansion of the master equation

In this section, we derive a master equation for the probability $P_t(\sigma)$ to observe a T-cell configuration $\sigma \in \{0, 1\}^N$ at time t , from the stochastic update rule (14) and we will use it to derive equations for the time evolution of the macroscopic variables $a(\sigma)$ and $m(\sigma)$. Denoting by $\mathcal{P}(x) = \int_{-\infty}^x dz P(z)$ the cumulative distribution function of the noise distribution $P(z)$, the likelihood to observe σ_i at time $t + \Delta$, given the T-cell configuration σ' at the earlier time step t , is, for any symmetric distribution $P(z) = P(-z)$,

$$P(\sigma_i, t + \Delta | \sigma', t) = \mathcal{P}(z \leq (2\sigma_i - 1)\beta (\eta_i \xi_i p(t) + (1 - \eta_i) \xi_i c(t)m(\sigma') - \phi(t))). \tag{49}$$

For the Glauber choice $\mathcal{P}(x) = \frac{1}{2}(1 + \tanh \frac{x}{2})$, the probability that T-cell i changes, in a single time step, its state at time t is

$$W_i^t(\sigma) = P_t(F_i \sigma | \sigma) = \frac{1}{2} \left(1 + (2\sigma_i - 1) \tanh \left(\frac{\beta h_i(t, \sigma)}{2} \right) \right) \tag{50}$$

where we have defined the ‘flip’ operator F_i such that $F_i \sigma = (\sigma_1, \dots, 1 - \sigma_i, \dots, \sigma_N)$ and $h_i(t, \sigma) = \eta_i \xi_i p(t) + (1 - \eta_i) \xi_i c(t)m(\sigma) - \phi(t)$. Assuming that the update of T-cells is sequential, i.e. at each time step one T-cell i , drawn at random, is updated with likelihood $W_i^t(\sigma)$, one obtains, for $\Delta = 1/N$ and N large, the following master equation

$$\partial_t P_t(\sigma) = \sum_i [P_t(F_i \sigma) W_i^t(F_i \sigma) - P_t(\sigma) W_i^t(\sigma)]. \tag{51}$$

From the master equation, the time evolution of the macroscopic variables can be retrieved using the Kramers-Moyal (KM) expansion. To perform this expansion we note that we can define the time-dependent probability distribution of the macroscopic variables as

$$P_t(a, m) = \sum_{\sigma} P_t(\sigma) \delta(a - a(\sigma)) \delta(m - m(\sigma)) \tag{52}$$

from which the master equation tells us,

$$\partial_t P_t(a, m) = \sum_{\sigma} \delta(a - a(\sigma)) \delta(m - m(\sigma)) [P_t(F_i \sigma) W_i^t(F_i \sigma) - P_t(\sigma) W_i^t(\sigma)]. \tag{53}$$

Defining $\mathbf{\Omega}(\boldsymbol{\sigma}) = (m(\boldsymbol{\sigma}), a(\boldsymbol{\sigma}))$ and relabelling the first term in our sum with $F_i\boldsymbol{\sigma} \rightarrow \boldsymbol{\sigma}$ we have

$$\partial_t P(\mathbf{\Omega}) = \sum_{\boldsymbol{\sigma}} P_t(\boldsymbol{\sigma}) W_i^t(\boldsymbol{\sigma}) [\delta(\mathbf{\Omega} - \mathbf{\Omega}(F_i\boldsymbol{\sigma})) - \delta(\mathbf{\Omega} - \mathbf{\Omega}(\boldsymbol{\sigma}))]. \tag{54}$$

We now define the change in the macroscopic parameter Ω_μ caused by a flip in a single T-cell i as $\Delta_{i\mu}(\boldsymbol{\sigma}) = \Omega_\mu(F_i\boldsymbol{\sigma}) - \Omega_\mu(\boldsymbol{\sigma})$ such that $\Delta_{i0}(\boldsymbol{\sigma}) = m(F_i\boldsymbol{\sigma}) - m(\boldsymbol{\sigma}) = \frac{1}{V}(1 - 2\sigma_i)\eta_i\xi_i$ and $\Delta_{i1}(\boldsymbol{\sigma}) = a(F_i\boldsymbol{\sigma}) - a(\boldsymbol{\sigma}) = \frac{1}{V}(1 - 2\sigma_i)\xi_i$. The KM expansion can then be carried out in powers of $\Delta_{i\mu}(\boldsymbol{\sigma})$,

$$\begin{aligned} \partial_t P(\mathbf{\Omega}) &= \sum_i \sum_{\boldsymbol{\sigma}} W_i^t(\boldsymbol{\sigma}) P_t(\boldsymbol{\sigma}) \left[- \sum_{\mu} \frac{\partial^2}{\partial \Omega_\mu^2} \delta[\mathbf{\Omega} - \mathbf{\Omega}(\boldsymbol{\sigma})] \Delta_{i\mu}(\boldsymbol{\sigma}) \right. \\ &\quad \left. + \frac{1}{2} \sum_{\mu\nu} \frac{\partial^2}{\partial \Omega_\mu \partial \Omega_\nu} \delta[\mathbf{\Omega} - \mathbf{\Omega}(\boldsymbol{\sigma})] \Delta_{i\mu}(\boldsymbol{\sigma}) \Delta_{i\nu}(\boldsymbol{\sigma}) + \dots \right]. \end{aligned} \tag{55}$$

A special case where the dynamical equations close is found when $\sum_i W_i^t(\boldsymbol{\sigma}) \Delta_{i\mu} = F_\mu^t(\mathbf{\Omega}(\boldsymbol{\sigma}), \dots)$, where F_μ^t is some function that depends on the microscopic variable $\boldsymbol{\sigma}$, through the macroscopic variables only, $\mathbf{\Omega}(\boldsymbol{\sigma})$. To this end we evaluate $\sum_i W_i(\boldsymbol{\sigma}) \Delta_{i\mu}(\boldsymbol{\sigma})$ for the cases $\mu = 0, 1$,

$$\begin{aligned} &\sum_i W_i^t(\boldsymbol{\sigma}) \Delta_{i0}(\boldsymbol{\sigma}) \\ &= \sum_i \frac{1}{2} \left(1 + (1 - 2\sigma_i) \tanh\left(\frac{\beta h_i(t, \boldsymbol{\sigma})(t, \boldsymbol{\sigma})}{2}\right) \right) \frac{1}{V} (1 - 2\sigma_i) \eta_i \xi_i \end{aligned} \tag{56}$$

$$= -m(\boldsymbol{\sigma}) + \frac{1}{2V} \sum_i \left(1 + \tanh\left(\frac{\beta}{2} (\eta_i \xi_i p(t) + (1 - \eta_i) \xi_i c(t) m(\boldsymbol{\sigma}) - \phi(t))\right) \right) \eta_i \xi_i \tag{57}$$

$$= F_0^t(\mathbf{\Omega}(\boldsymbol{\sigma}), \mathbf{c}) \tag{58}$$

and similarly,

$$\begin{aligned} &\sum_i W_i^t(\boldsymbol{\sigma}) \Delta_{i1}(\boldsymbol{\sigma}) \\ &= \sum_i \frac{1}{2} \left(1 + (1 - 2\sigma_i) \tanh\left(\frac{\beta h_i(t, \boldsymbol{\sigma})}{2}\right) \right) \frac{1}{V} (1 - 2\sigma_i) \xi_i \end{aligned} \tag{59}$$

$$= -a(\boldsymbol{\sigma}) + \frac{1}{2V} \sum_i \left(1 + \tanh\left(\frac{\beta}{2} (\eta_i \xi_i p(t) + (1 - \eta_i) \xi_i c(t) m(\boldsymbol{\sigma}) - \phi(t))\right) \right) \xi_i \tag{60}$$

$$= F_1^t(\mathbf{\Omega}(\boldsymbol{\sigma}), \mathbf{c}) \tag{61}$$

where we have denoted $\mathbf{c} = (c, b, p)$ and note that from Eqs. (15)–(16), \mathbf{c} only depends on σ through $\Omega(\sigma)$. Indeed, it is the case that

$$\sum_i W_i^t(\sigma) \Delta_{i\mu}(\sigma) = F_\mu^t(\Omega(\sigma), \mathbf{c}) \tag{62}$$

with no explicit dependence on σ . By substituting Eq. (62) into (55) the sum over σ can be taken; this constrains $\Omega_\mu(\sigma) = \Omega_\mu$ and yields,

$$\partial_t P_t(\Omega) = - \sum_{\mu=0}^1 \frac{\partial}{\partial \Omega_\mu} [P(\Omega) F_\mu^t(\Omega, \mathbf{c})] + \dots \tag{63}$$

Higher order terms in the KM expansion are shown to be proportional to V^{-d} , where $d \geq 1$, and are therefore negligible in the limit that V is large. Equation (63) in this limit reduces to the Liouville equation

$$\frac{d\Omega}{dt} = \mathbf{F}^t(\Omega, \mathbf{c}) \tag{64}$$

which is otherwise written,

$$\frac{dm}{dt} = -m + \frac{1}{2V} \sum_i \eta_i \xi_i \left(1 + \tanh \left(\frac{\beta}{2} (\eta_i \xi_i p + (1 - \eta_i) \xi_i cm - \phi(t)) \right) \right) \tag{65}$$

$$\frac{da}{dt} = -a + \frac{1}{2V} \sum_i \xi_i \left[1 + \tanh \left(\frac{\beta}{2} (\eta_i \xi_i p + (1 - \eta_i) \xi_i cm - \phi(t)) \right) \right]. \tag{66}$$

To simplify these equations further, we make use of the empirical joint distribution of η and ξ ,

$$P(\eta, \xi) \hat{=} \frac{1}{N} \sum_j \delta_{\eta, \eta_j} \delta_{\xi, \xi_j} \tag{67}$$

with averages over this distribution then defined as

$$\langle \dots \rangle_{\eta, \xi} = \sum_{\eta, \xi} \dots P(\eta, \xi). \tag{68}$$

The macroscopic dynamics are then summarised by the following ODEs,

$$\frac{dm}{dt} = -m + \frac{\rho}{2} \left\langle \eta \xi \left[1 + \tanh \left(\frac{\beta}{2} (\eta \xi p + (1 - \eta) \xi cm - \phi(t)) \right) \right] \right\rangle_{\eta, \xi} \tag{69}$$

$$\frac{da}{dt} = -a + \frac{\rho}{2} \left\langle \xi \left[1 + \tanh \left(\frac{\beta}{2} (\eta \xi p + (1 - \eta) \xi cm - \phi(t)) \right) \right] \right\rangle_{\eta, \xi}. \tag{70}$$

This corresponds to a mean-field description of the evolution of the stochastic variables $\Omega_\mu(\sigma)$. For large but finite values of V , $\Omega_\mu(\sigma)$ will fluctuate about its mean value $\Omega_\mu = \langle \Omega_\mu(\sigma) \rangle_\sigma$ with fluctuations of order $\sqrt{\Delta_{i\mu}} = \mathcal{O}(V^{-\frac{1}{2}})$.

References

- Agliari E, Annibale A, Barra A, Coolen ACC, Tantari D (2013) Immune networks: multi-tasking capabilities near saturation. *J Phys A: Math Theor.* <https://doi.org/10.1088/1751-8113/46/41/415003>
- Aleksic M, Dushek O, Zhang H, Shenderov E, Chen JL, Cerundolo V, Coombs D, van der Merwe PA (2010) Dependence of T cell antigen recognition on T cell receptor-peptide MHC confinement time. *Immunity* 32(2):163–174. <https://doi.org/10.1016/j.immuni.2009.11.013>
- Allard M, Couturaud B, Carretero-Iglesia L, Duong MN, Schmidt J, Monnot GC, Romero P, Speiser DE, Hebeisen M, Rufer N (2017) TCR-ligand dissociation rate is a robust and stable biomarker of CD8+ T cell potency. *JCI Insight.* <https://doi.org/10.1172/jci.insight.92570>
- Annibale A, Dziobek-Garrett LA, Tari H (2018) The role of the T-helper/T-suppressor ratio in the adaptive immune response: a dynamical model. *J Phys A: Math Theor.* <https://doi.org/10.1088/1751-8121/aed5e>
- Bartolucci S, Mozeika A, Annibale A (2016) The role of idiotypic interactions in the adaptive immune system: A belief-propagation approach. *J Stat Mech: Theory Exp.* <https://doi.org/10.1088/1742-5468/2016/08/083402>
- Brentjens RJ, Davila ML, Riviere I, Park J, Wang X, Cowell LG, Bartido S, Stefanski J, Taylor C, Olszewska M, Borquez-Ojeda O, Qu J, Wasielewska T, He Q, Bernal Y, Rijo IV, Hedvat C, Kobos R, Curran K, Steinherz P, Jurcic J, Rosenblat T, Maslak P, Frattini M, Sadelain M (2013) CD19-targeted T cells rapidly induce molecular remissions in adults with chemotherapy-refractory acute lymphoblastic leukemia. *Sci Trans Med* 5(177):177ra38. <https://doi.org/10.1126/scitranslmed.3005930>
- Burroughs NJ, Van Der Merwe PA (2007) Stochasticity and spatial heterogeneity in T-cell activation. *Immunol Rev* 216(1):69–80. <https://doi.org/10.1111/j.1600-065X.2006.00486.x>
- Chakraborty AK, Košmrlj A (2010) Statistical mechanical concepts in immunology. *Annu Rev Phys Chem* 61(1):283–303. <https://doi.org/10.1146/annurev.physchem.59.032607.093537>
- Coolen A, Ruijgrok TW (1988) Image evolution in hopfield networks. *Phys Rev A* 38(8):4253
- Coolen A, Sherrington D (1993) Dynamics of fully connected attractor neural networks near saturation. *Phys Rev Lett* 71(23):3886
- Diederichsen ACP, v B Hjelmberg J, Christensen PB, Zeuthen J, Fenger C (2003) Prognostic value of the CD4+/CD8+ ratio of tumour infiltrating lymphocytes in colorectal cancer and HLA-DR expression on tumour cells. *Cancer Immunol Immunother* 52(7):423–428. <https://doi.org/10.1007/s00262-003-0388-5>
- Dritschel H, Waters SL, Roller A, Byrne HM (2018) A mathematical model of cytotoxic and helper T cell interactions in a tumour microenvironment. *Letters Biomath* 10(1080/23737867):1465863
- Dunn GP, Old LJ, Schreiber RD (2004) The three Es of cancer immunoeediting. *Annu Rev Immunol* 22(1):329–360. <https://doi.org/10.1146/annurev.immunol.22.012703.104803>
- Eftimie R, Eftimie G (2018) Tumour-associated macrophages and oncolytic virotherapies: a mathematical investigation into a complex dynamics. *Letters Biomath* 5(sup1):S6–S35. <https://doi.org/10.1080/23737867.2018.1430518>
- Garcia-Lora A, Algarra I, Garrido F (2003) MHC class I antigens, immune surveillance, and tumor immune escape. <https://doi.org/10.1002/jcp.10290>
- Hodi FS, O'Day SJ, McDermott DF, Weber RW, Sosman JA, Haanen JB, Gonzalez R, Robert C, Schadendorf D, Hassel JC, Akerley W, van den Eertwegh AJ, Lutzky J, Lorigan P, Vaubel JM, Linette GP, Hogg D, Ottensmeier CH, Lebbé C, Peschel C, Quirt I, Clark JI, Wolchok JD, Weber JS, Tian J, Yellin MJ, Nichol GM, Hoos A, Urba WJ (2010) Improved Survival with Ipilimumab in Patients with Metastatic Melanoma. *N Engl J Med* 363(8):711–723. <https://doi.org/10.1056/NEJMoa1003466>
- Irvine DJ, Purbhoo MA, Krogsgaard M, Davis MM (2002) Direct observation of ligand recognition by T cells. *Nature* 419(6909):845–849. <https://doi.org/10.1038/nature01076>
- Jordanova ES, Gorter A, Ayachi O, Prins F, Durrant LG, Kenter GG, van der Burg SH, Fleuren GJ (2008) Human Leukocyte Antigen Class I, MHC Class I chain-related molecule A, and CD8+/Regulatory T-

- cell ratio: which variable determines survival of cervical cancer patients? *Clin Cancer Res* 14(7):2028–2035. <https://doi.org/10.1158/1078-0432.CCR-07-4554>
- Kakarla S, Gottschalk S (2014) CAR T cells for solid tumors. *Cancer J* 20(2):151–155. <https://doi.org/10.1097/PPO.000000000000032>
- Kochenderfer JN, Dudley ME, Kassim SH, Somerville RPT, Carpenter RO, Stetler-Stevenson M, Yang JC, Phan GQ, Hughes MS, Sherry RM, Raffeld M, Feldman S, Lu L, Li YF, Ngo LT, Goy A, Feldman T, Spaner DE, Wang ML, Chen CC, Kranick SM, Nath A, Nathan DAN, Morton KE, Toomey MA, Rosenberg SA (2014) Chemotherapy-refractory diffuse large B-cell lymphoma and indolent B-cell malignancies can be effectively treated with autologous T cells expressing an anti-CD19 chimeric antigen receptor. *J Clin Oncol* 33:540–549. <https://doi.org/10.1200/JCO.2014.56.2025>
- Kuznetsov V, Makalkin I, Taylor M, Perelson A (1994) Nonlinear dynamics of immunogenic tumors: parameter estimation and global bifurcation analysis. *Bull Math Biol* 56(2):295–321. [https://doi.org/10.1016/S0092-8240\(05\)80260-5](https://doi.org/10.1016/S0092-8240(05)80260-5)
- Leach DR, Krummel MF, Allison JP (1996) Enhancement of antitumor immunity by CTLA-4 blockade. *Science* 271(5256):1734–1736. <https://doi.org/10.1126/science.271.5256.1734>
- Li J, Yin W, Jing Y, Kang D, Yang L, Cheng J, Yu Z, Peng Z, Li X, Wen Y et al (2019) The coordination between b cell receptor signaling and the actin cytoskeleton during b cell activation. *Front Immunol* 9:3096
- Lipniacki T, Hat B, Faeder JR, Hlavacek WS (2008) Stochastic effects and bistability in T cell receptor signaling. *J Theor Biol* 254(1):110–122. <https://doi.org/10.1016/j.jtbi.2008.05.001>
- Lucia U, Maino G (2002) Thermodynamical analysis of the dynamics of tumor interaction with the host immune system. *Physica A* 313(3–4):569–577. [https://doi.org/10.1016/S0378-4371\(02\)00980-9](https://doi.org/10.1016/S0378-4371(02)00980-9)
- Madjd Z, Spendlove I, Pinder SE, Ellis IO, Durrant LG (2005) Total loss of MHC class I is an independent indicator of good prognosis in breast cancer. *Int J Cancer* 117(2):248–255. <https://doi.org/10.1002/ijc.21163>
- McDermott DF, Drake CG, Sznol M, Choueiri TK, Powderly JD, Smith DC, Brahmer JR, Carvajal RD, Hammers HJ, Puzanov I, Hodi FS, Kluger HM, Topalian SL, Pardoll DM, Wigginton JM, Kollia GD, Gupta A, McDonald D, Sankar V, Sosman JA, Atkins MB (2015) Survival, durable response, and long-term safety in patients with previously treated advanced renal cell carcinoma receiving Nivolumab. *J Clin Oncol* 33(18):2013–2020. <https://doi.org/10.1200/JCO.2014.58.1041>
- Ménard S, Tomasic G, Casalini P, Balsari A, Pilotti S, Cascinelli N, Salvadori B, Colnaghi MI, Rilke F, Büchler MW, Schmidt J (1997) Lymphoid infiltration as a prognostic variable for early-onset breast carcinomas. *Clin Cancer Res Off J Am Assoc Cancer Res* 3(5):817–9
- Mora T, Walczak AM, Bialek W, Callan CG (2010) Maximum entropy models for antibody diversity. *Proc Natl Acad Sci USA* 107(12):5405–5410. <https://doi.org/10.1073/pnas.1001705107>. [arXiv:0912.5175](https://arxiv.org/abs/0912.5175)
- Nishimori H, Nakamura T, Shiino M (1990) Retrieval of spatio-temporal sequence in asynchronous neural network. *Phys Rev A* 41(6):3346
- Nunes C, Wong R, Mason M, Fegan C, Man S, Pepper C (2012) Expansion of a CD8th PD-1 th Replicative senescence phenotype in early stage CLL patients is associated with inverted CD4:CD8 ratios and disease progression. *Human Cancer Biol*. <https://doi.org/10.1158/1078-0432.CCR-11-2630>
- Olsson J, Wikby A, Johansson B, Löfgren S, Nilsson BO, Ferguson FG (2001) Age-related change in peripheral blood T-lymphocyte subpopulations and cytomegalovirus infection in the very old: The Swedish longitudinal OCTO immune study. *Mech Ageing Dev* 121(1–3):187–201. [https://doi.org/10.1016/S0047-6374\(00\)00210-4](https://doi.org/10.1016/S0047-6374(00)00210-4)
- Perelson AS, Weisbuch G (1997) Immunology for physicists. *Rev Mod Phys* 69(4):1219–1267. <https://doi.org/10.1103/revmodphys.69.1219>
- Platt CD, Ma JK, Chalouni C, Ebersold M, Bou-Reslan H, Carano RA, Mellman I, Delamarre L (2010) Mature dendritic cells use endocytic receptors to capture and present antigens. *Proc Natl Acad Sci USA* 107(9):4287–4292. <https://doi.org/10.1073/pnas.0910609107>
- Restifo NP, Dudley ME, Rosenberg SA (2012). Adoptive immunotherapy for cancer: Harnessing the T cell response. <https://doi.org/10.1038/nri3191>
- Robert P, Aleksic M, Dushek O, Cerundolo V, Bongrand P, Van Der Merwe PA (2012) Kinetics and mechanics of two-dimensional interactions between T cell receptors and different activating ligands. *Biophys J* 102(2):248–257. <https://doi.org/10.1016/j.bpj.2011.11.4018>
- Ryschich E, Nötzel T, Hinz U, Autschbach F, Ferguson J, Simon I, Weitz J, Fröhlich B, Klar E, Büchler M, Schmidt J (2005) Control of T-cell-mediated immune response by HLA class I in human pancreatic carcinoma. *Clin Cancer Res Off J Am Assoc Cancer Res* 11(2 Pt 1):498–504

- Sato E, Olson SH, Ahn J, Bundy B, Nishikawa H, Qian F, Jungbluth AA, Frosina D, Gnjatich S, Ambrosone C, Kepner J, Odunsi T, Ritter G, Lele S, Chen YT, Ohtani H, Old LJ, Odunsi K (2005) Intraepithelial CD8+ tumor-infiltrating lymphocytes and a high CD8+/regulatory T cell ratio are associated with favorable prognosis in ovarian cancer. *Proc Natl Acad Sci* 102(51):18538–18543. <https://doi.org/10.1073/pnas.0509182102>
- Scheper W, Kelderman S, Fanchi LF, Linnemann C, Bendle G, de Rooij MA, Hirt C, Mezzadra R, Slagter M, Dijkstra K, Kluin RJ, Snaebjornsson P, Milne K, Nelson BH, Zijlmans H, Kenter G, Voest EE, Haanen JB, Schumacher TN (2019) Low and variable tumor reactivity of the intratumoral TCR repertoire in human cancers. *Nat Med* 25(1):89–94. <https://doi.org/10.1038/s41591-018-0266-5>
- Serrano-Villar S, Sainz T, Lee SA, Hunt PW, Sinclair E, Shacklett BL, Ferre AL, Hayes TL, Somsouk M, Hsue PY, Van Natta ML, Meinert CL, Lederman MM, Hatano H, Jain V, Huang Y, Hecht FM, Martin JN, McCune JM, Moreno S, Deeks SG (2014) HIV-infected individuals with Low CD4/CD8 ratio despite effective antiretroviral therapy exhibit altered T cell subsets, heightened CD8+ T cell activation, and increased risk of non-AIDS morbidity and mortality. *PLoS Pathogens*. <https://doi.org/10.1371/journal.ppat.1004078>
- Sevcíková L, Hunáková L, Chorváth B, Turzová M, Boljesíková E (1992) T-lymphocyte subsets (CD4/CD8 ratio) in breast cancer patients. *Neoplasma* 39(4):219–22
- Sheu BC, Hsu SM, Ho HN, Lin RH, Torng PL, Huang SC (1999) Reversed CD4/CD8 ratios of tumor-infiltrating lymphocytes are correlated with the progression of human cervical carcinoma. *Cancer* 86(8):1537–1543. [https://doi.org/10.1002/\(SICI\)1097-0142\(19991015\)86:8<1537::AID-CNCR21>3.0.CO;2-D](https://doi.org/10.1002/(SICI)1097-0142(19991015)86:8<1537::AID-CNCR21>3.0.CO;2-D)
- Sheu BC, Kuo WH, Chen RJ, Huang SC, Chang KJ, Chow SN (2008) Clinical significance of tumor-infiltrating lymphocytes in neoplastic progression and lymph node metastasis of human breast cancer. *Breast* 17(6):604–610. <https://doi.org/10.1016/j.breast.2008.06.001>
- Simpson JAD, Al-Attar A, Watson NFS, Scholefield JH, Ilyas M, Durrant LG (2010) Intratumoral T cell infiltration, MHC class I and STAT1 as biomarkers of good prognosis in colorectal cancer. *Gut* 59(7):926–933. <https://doi.org/10.1136/gut.2009.194472>
- Sompolinsky H, Crisanti A, Sommers HJ (1988) Chaos in random neural networks. *Phys Rev Lett* 61(3):259
- Tancini G, Barni S, Rescaldani R, Fiorelli G, Viviani S, Lissoni P (1990) Analysis of t helper and suppressor lymphocyte subsets in relation to the clinical stage of solid neoplasms. *Oncology* 47(5):381–384
- Taylor JM, Fahey JL, Detels R, Giorgi JV (1989) Cd4 percentage, cd4 number, and cd4:cd8 ratio in hiv infection: Which to choose and how to use. *J Acquir Immune Defic Syndr* 2(2):114–124
- Tian S, Maile R, Collins EJ, Frelinger JA (2007) CD8 + T cell activation is governed by TCR-Peptide/MHC affinity, not dissociation rate. *J Immunol* 179(5):2952–2960. <https://doi.org/10.4049/jimmunol.179.5.2952>
- Tkach K, Altan-Bonnet G (2013) T cell responses to antigen: Hasty proposals resolved through long engagements. <https://doi.org/10.1016/j.coi.2012.12.001>
- Turcotte S, Katz SC, Shia J, Jarnagin WR, Kingham TP, Allen PJ, Fong Y, D'Angelica MI, DeMatteo RP (2014) Tumor MHC class I expression improves the prognostic value of T-cell density in resected colorectal liver metastases. *Cancer Immunol Res* 2(6):530–7. <https://doi.org/10.1158/2326-6066.CIR-13-0180>
- Watson NF, Ramage JM, Madjd Z, Spendlove I, Ellis IO, Scholefield JH, Durrant LG (2006) Immunosurveillance is active in colorectal cancer as downregulation but not complete loss of MHC class I expression correlates with a poor prognosis. *Int J Cancer* 118(1):6–10. <https://doi.org/10.1002/ijc.21303>
- Wedagedera JR, Burroughs NJ (2006) T-cell activation: a queuing theory analysis at low agonist density. *Biophys J* 91(5):1604–1618. <https://doi.org/10.1529/biophysj.105.066001>
- Wikby A, Maxson P, Olsson J, Johansson B, Ferguson FG (1998) Changes in CD8 and CD4 lymphocyte subsets, T cell proliferation responses and non-survival in the very old: The Swedish longitudinal OCTO-immune study. *Mech Ageing Dev Elsevier* 102:187–198. [https://doi.org/10.1016/S0047-6374\(97\)00151-6](https://doi.org/10.1016/S0047-6374(97)00151-6)